

# New Developments in the Search for the Topology of the Universe

Jean-Philippe Uzan<sup>1</sup>, Roland Lehoucq<sup>2</sup> and Jean-Pierre Luminet<sup>3</sup>

(1) *Département de Physique Théorique, Université de Genève,  
24 quai E. Ansermet, CH-1211 Geneva (Switzerland)*

(2) *CE-Saclay, DSM/DAPNIA/Service d'Astrophysique,  
F-91191 Gif sur Yvette cedex (France)*

(3) *Département d'Astrophysique Relativiste et de Cosmologie,  
Observatoire de Paris, UPR 176, CNRS, F-92195 Meudon (France).*

Email: uzan@amorgos.unige.ch, roller@discovery.saclay cea.fr, jean-pierre.luminet@obspm.fr

**Abstract.** Multi-connected Universe models with space identification scales smaller than the size of the observable universe produce topological images in the catalogs of cosmic sources. In this review, we present the recent developments for the search of the topology of the universe focusing on three dimensional methods. We present the crystallographic method, we give a new lower bound on the size of locally Euclidean multi-connected universe model of  $3000 h^{-1}$  Mpc based on this method and a quasar catalog, we discuss its successes and failures, and the attempts to generalise it. We finally introduce a new statistical method based on a collecting correlated pair (CCP) technique.

## 1. BASICS

### 1.1. Historical elements

In the standard cosmological framework, the universe is described by a Friedmann-Lemaître solution, the spatial sections of which being usually assumed to be simply-connected. Einstein equations being local, they allow us to determine the local geometry but they give no complete information about the global structure of the universe, i.e. about its topology, even if the geometry constrains to some extent the topology. This was pointed out by Friedmann himself just after he proposed its cosmological solution [1]. The indeterminacy about the global topology of the cosmological solutions was raised out as soon as Einstein proposed the first cosmological solution of his equations ; the Einstein static universe assumed spatial sections with the topology of the hypersphere  $S^3$  [2], although de Sitter stressed that the same geometry could admit as well the projective space  $P^3 = S^3/Z^2$  as spatial sections [3]. These two solutions were locally identical (same metric) but differed by their topology, i.e. by the choice of boundary conditions.

Many arguments were then advanced in favour of a simply-connected universe, such as the simplicity or economy principle stating that one should introduce as few parameters as possible in physical modelling. Indeed, such an argument is very

unclear. There has been some tendency to favor spaces with finite volume. The eternal and infinite space of Newtonian physics was for instance leading to logical difficulties such as the Olbers paradox [4], and the finite cosmological solution proposed by Einstein in 1917 was received as a smart way of solving such paradoxes. The Mach's principle [5, 6] based on the idea that the local inertia is determined by the distribution of masses in the whole universe, also tends to favor universes with a finite volume. If space is simply-connected then it is finite if and only if it is locally elliptic, whereas if multi-connected it can also be locally hyperbolic or Euclidean. It has also been argued that infinite spaces were unaesthetic since "all phenomenon with a non vanishing probability must happen somewhere else" [7, 8]. This argument was used by Ellis to conclude that if space was infinite then one can avoid the former conclusion by dropping the assumption of spatial homogeneity and by arguing that we were living in a particular place of the universe [8]. To finish, many arguments coming from some ideas in quantum cosmology are in favor of a finite volume space [9, 10, 11, 12]. Indeed, none of these arguments can help us to determine the shape and size of our universe. So, we are lead to the question, can we detect or constrain observationally the topology of our universe ?

Astonishingly enough, our century has on one hand seen the birth of the geometrical description of the universe and of a non static curved spacetime. On the other, mathematicians have developed the classification of 3D-manifolds. The first motivation came from crystallography, which lead to the classification of Euclidean 3D-manifolds [13, 14] and was achieved in 1934 [15]. The classification of locally elliptic 3-manifold was set by F. Klein [16] and W. Killing [17] and solved by J.A. Wolf in 1960 [18]. The classification of locally hyperbolic manifold was started in the 70's by W. Thurston [19, 20] and is not yet achieved [21, 22, 23]. Thus both elements necessary to answer the question of cosmic topology were developed at the same time without interacting so much. For more details concerning this interesting modern quest, one can see [24, 25, 26, 27].

## 1.2. Mathematical elements

In relativistic cosmology, our universe is described by a globally hyperbolic 4-manifold  $\mathcal{M} = \Sigma \times R$  [28, 29], where the spatial sections  $\Sigma$  are homogeneous and isotropic Riemannian 3-manifolds. From a topological point of view, it is convenient to describe such a manifold by its fundamental polyhedron (hereafter FP), which is convex. Its faces are associated by pairs through the elements of a holonomy group  $\Gamma$  which is acting freely and discontinuously on  $\Sigma$  (see [30, 31, 32] for mathematical definitions and [33, 34, 35] for an introduction to topology in the cosmological context). The holonomy group is isomorphic to the fundamental group  $\pi_1(\Sigma)$ . Using the property (see e.g. [32]):

$$\pi_1(\mathcal{M}) = \pi_1(\Sigma \times R) \sim \pi_1(R) \times \pi_1(\Sigma) \sim \pi_1(\Sigma), \quad (1)$$

we deduce that the study of the topology of the universe reduces to the study of the topology of its spatial sections.

What are the allowed homogeneous 3-manifolds usable in cosmology ? According to the sign of the spatial curvature  $K$ , the universal covering space of the spatial sections (which will be referred to as  $\tilde{\Sigma}$ ) can be described by the Euclidean space  $E^3$ , the hypersphere  $S^3$  or the 3-hyperboloid  $H^3$  if  $K$  vanishes, is positive or negative

respectively. Thus, the homogeneous and isotropic 3-manifolds will be of the form

$$E^3/\Gamma, \quad S^3/\Gamma \quad \text{and} \quad H^3/\Gamma. \quad (2)$$

Let us just summarize some of the properties of each family and also introduce  $G$ , the full isometry group of  $\tilde{\Sigma}$  keeping the metric invariant. Indeed  $\Gamma$  will be a discrete sub-group of  $G$ .

- (i) locally Euclidean 3-manifolds: The covering space in the Euclidean space  $\tilde{\Sigma} = E^3$  and the isometry group is  $G = R^3 \times SO(3)$ . The metric can be written under the form

$$ds^2 = a^2(\eta) \{ -d\eta^2 + d\chi^2 + \chi^2 d\Omega \}, \quad (3)$$

where  $\eta$  is the conformal time,  $a(\eta)$  the scale factor,  $\chi$  the radial coordinate and  $d\Omega$  the unit solid angle. The generator of  $\Gamma$  are the identity, the translations, the reflexions and the helicoidal motions.

These transformations generate 18 different spaces [18] among which 17 are multi-connected and correspond to the 17 crystallographic groups [13]. 10 spaces are compact and among them 6 are orientable. The description of these spaces can be found in e.g. [33].

- (ii) locally elliptic 3-manifolds : The covering space in the elliptic space  $\tilde{\Sigma} = S^3$  and the isometry group is  $G = SO(4)$ . The metric can be written as

$$ds^2 = a^2(\eta) \{ -d\eta^2 + d\chi^2 + \sin^2 \chi d\Omega \}. \quad (4)$$

With the curvature radius as unit length, the volume of the hypersphere is

$$\text{Vol}(S^3) = \int_0^\pi 4\pi \sin^2 \chi d\chi = 2\pi^2. \quad (5)$$

Wolf [18] gives an exhaustive description of the allowed discrete groups  $\Gamma$ . They are the cyclic groups of order  $p$  ( $p \geq 2$ ), the dihedral groups of order  $2m$ , and the symmetry groups of the tetrahedron, octaedron and icosahedron.

If we denote  $|\Gamma|$  the order of the holonomy group, it is straightforward to show that

$$\text{Vol}(S^3/\Gamma) = 2\pi^2/|\Gamma|, \quad (6)$$

which tells us that the volume of an elliptic manifold is a topological invariant (degenerate since two different groups with same order will have same volume).

- (iii) locally hyperbolic 3-manifolds: The covering space in the hyperbolic space  $\tilde{\Sigma} = H^3$  and the isometry group is  $G = PSL(2, C) \equiv SL(2, C)/Z_2$ . The metric can be written as

$$ds^2 = a^2(\eta) \{ -d\eta^2 + d\chi^2 + \sinh^2 \chi d\Omega \}. \quad (7)$$

The classification of compact hyperbolic manifolds is not achieved yet and we will just describe two of them and give some useful properties. This classification

relies on the rigidity theorem [40, 41] stating that the geometry is fixed by the topology, a consequence of which being that the volume and other characteristic lengths are topological invariants, so that

$$\pi_1(X) \sim \pi_1(Y) \iff \text{Vol}(X) = \text{Vol}(Y). \quad (8)$$

It has also been shown that there is a minimal allowed volume [42]

$$\text{Vol}(\Sigma) \geq \text{Vol}_{\min} = 0.166. \quad (9)$$

We also define the outside radius  $r_+$ , the radius of the smallest geodesic ball that contains the FP, the inside radius  $r_-$ , the radius of the biggest geodesic ball contained in the FP, and the injectivity radius  $r_{\text{inj}}$ , half the length of the shortest closed geodesic.  $r_+$ ,  $r_-$  and  $r_{\text{inj}}$  are altogether topological invariants.

The classification and the description of the known compact hyperbolic manifolds can be obtained by using the software *SnapPea* [39] which provides the FP, the generators of the holomy group and the characteristic lengths. Examples of such manifolds can be found in e.g. [33]. Here we mention for a later use a manifold of special interest, the Weeks space [37], which is the smallest known compact hyperbolic manifold. Its FP has 18 faces and its geometrical characteristics are

$$\text{Vol} = 0.94272, r_+ = 0.7525, r_- = 0.5192, r_{\text{inj}} = 0.2923 \quad (10)$$

### 1.3. Physical and observational introduction

At the time being, two classes of methods to detect and/or constrain the topology of the spatial sections of our universe have been proposed and investigated. They use two classes of cosmological observations, namely the 2D cosmic microwave background data and the 3D catalogs of discrete sources.

- (i) 2D-methods: The cosmic microwave background is composed of all the photons emitted during the decoupling period between matter and radiation at a redshift of  $z \sim 1100$ . It is observed as a black body with a temperature of 2.7 K with small fluctuations of order  $10^{-5}$ . The temperature anisotropies reflect the small inhomogeneities that ultimately lead to the observed structures in the universe.

When studying these anisotropies in a multi-connected universe, one has to take into account the fact that we are in a compact manifold and thus that the wavelengths must be discretized. Stevens *et al.* [47] showed that in a cubic hypertorus one should see a cut-off in the two-point correlation function if  $L/R_H \leq 0.8$ . This analysis was then generalised to non cubic hypertorus [48] and to the six flat manifolds [50]. However, in compact hyperbolic manifolds there are super-curvature modes [19], which implies that no such cut-off exists [52, 53].

It has then been realised that the patterns on such an extended surface must be correlated if the universe is multi-connected. Levin *et al.* [51] studied these correlations in the flat manifolds and Cornish *et al.* [49] developed a topology independent method to look for a topological signature in the cosmic microwave background map as expected from the MAP and Planck satellites.

All these studies have been performed assuming that the small initial inhomogeneities were generated during an inflationary phase. There is however another process that could generate such inhomogeneities, namely topological defects produced during a symmetry breaking phase transition in the early universe. Uzan and Peter [54] showed that the topology implies a constraint on the topological defects network from which it was deduced [55] that there will be a cut-off in the angular power spectrum of the temperature anisotropies, the cut-off value depending only on the characteristic size of the universe and on the cosmological parameters. Note that such considerations also provide another method for constraining the topology, namely the observation of an extended defect at a redshift  $z$  will give a lower bound on the size of the universe.

In conclusion, at the moment 2D-methods constrain flat manifolds to  $L/R_H \leq 0.8$ , and there is no convincing constraint on compact hyperbolic manifolds [56]. Some powerful methods can be hoped to be used when high resolution cosmic microwave background maps are achieved.

- (ii) **3D-methods:** In the framework of pre-relativistic cosmology, it was already pointed out by Schwarzschild that if space is multi-connected, one could see multiple images of astronomical objects [43], whereas Friedmann [1] did the same in the framework of general relativity. All 3D-methods for testing the space topology are based on this fact. We shall develop their description in the following sections.

In these Proceedings, we describe the developments of the 3D-methods, from the Schwarzschild initial idea of the existence of multiple images of the same object, until its statistical implementation under the form of cosmic crystallography. We then carefully study the method and explain why, contrary to what was previously thought, it won't work in locally hyperbolic universes. We then present attempts to generalise it and finish by describing a new and promising "CCP" method. This will be exemplified by numerical simulations with depiction of color pictures in order to make the subject as clear as possible.

## 2. FROM THE ORIGINAL IDEA TO THE CRYSTALLOGRAPHIC METHOD

### 2.1. Initial idea

As stressed above, if space is multi-connected, one should see multiple "topological" images of the same object. This is illustrated on figure 1 where we have used a 2-D example. In the universal covering space, the spacetime trajectories of the different images ( $A, B, \dots$ ) of a given object will intersect the observer past light cone at different times ( $a, b, \dots$ ). The same object will then be seen at different stages of its evolution. Indeed in a 4D universe, these images will also be seen in different directions of the sky.

The question is indeed to find methods to implement such a property in order to detect or to put lower bounds on the size of the universe.

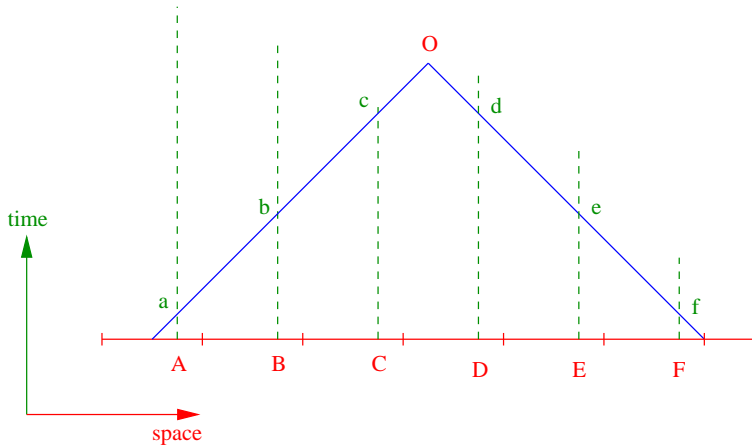


**Figure 1.** a  $1+1$  analogy of an multi-connected universe  $S^1 \times R$ . In the universal covering space, we have plotted the past light cone of the observer (blue), the trajectories (green) of different topological images (A-F) of a given object, assuming it is comoving, and the spacetime point (a-f) where they are observed.  $O$  will see them at different look-back times. Indeed in  $3+1$  dimension, he will also see them in different directions in the sky.

## 2.2. Multiple images of individual objects

Some specific objects have been tried to be recognised individually. An extensive description of these attempts can be found in [33] and we just stick to a brief description.

- Milky Way: Can we recognise our own Galaxy ? The maximum distance up to which we would be able to do that has been estimated as  $7.5 h^{-1}$  Mpc by Sokolov and Shvartsman [58] which gave the observational bound  $r_+ \geq 15 h^{-1}$  Mpc. Then, Fagundes and Wichoski [61] proposed that our galaxy was a quasar long ago but indeed, for physical reasons due to realistic quasar models, our Galaxy cannot have been a quasar in its past. Fagundes [71] also studied the occurrence of images of the Milky Way in the Best hyperbolic space model [74]. Presently, no source has been identified as an image of our own Galaxy.
- Galaxy clusters : Gott used the Coma cluster [62] has a candidate for the search of ghost images and obtained the bound  $r_+ \geq 60 h^{-1}$  Mpc. He also performed simulations in  $T^3$  to provide a pattern of clustering and a correlation function in agreement with observations of nearby galaxies. Roukema and Edge [46] proposed 3 candidates as ghost images for the Coma cluster. Further investigations are needed.

Sokoloff and Shvartsman [58] considered the Abell catalog of clusters and gave the bound  $r_+ \geq 600 h^{-1}$  Mpc in Euclidean space, whereas Demianski and Lapucha [60] searched unsuccessfully for opposite pairs in a catalog of 1889 clusters. Lehoucq *et al.* developed a statistical method that is presented below to obtain  $r_+ \geq 650 h^{-1}$  Mpc in Euclidean space and Fetisova *et al.* reported a spike about  $125 h^{-1}$  Mpc in the correlation function of rich clusters, but such an evidence does not necessarily supports multi-connectedness (see e.g. [33]).

- Quasars: Quasars occupy a large volume of the universe ( $z \simeq 3$ ). However, they are probably short-lived compared to the expected time necessary for a photon

to go around the universe. If  $\tau_q \simeq 10^9$  years, then one can hope to test topology on scale  $\sim r_+ \simeq c\tau_q$ . So, they are of interest even if  $\tau_q \simeq 10^8$  years. Paál [65] remarked that although individual quasars may have short lifetime, they may be part of larger associations which survive longer.

Roukema [45] tried to identify quintuplets and quadruplets of quasars in a catalog of 4554 quasars. He found 27 identifications whereas he found  $26 \pm 1$  identifications in simulations of a simply-connected universe. Fagundes [71] tried to discuss the redshift controversy in the Best [74] model.

Until now, the best bound obtained by 3D-methods was  $r_+ \geq 650 h^{-1} \text{Mpc}$  and hold only in Euclidean universe. There is still some observational room for the topologies of an hyperbolic universe, even on scales significantly shorter than the horizon radius.

All the methods trying to recognize a particular object suffer from the same major problems:

- (i) distance determination: catalogs give the angular position and the redshift. One has then to go from redshift space to real space, which depends on the knowledge of the cosmological constant and of the density parameter. This explained why most of the former studies were performed assuming  $\Omega_0 = 1, \Omega_\Lambda = 0$ . This point will be develop later.
- (ii) peculiar velocities: objects are not comoving, so that the position of their topological images are shifted. If their velocity is of order  $v_p \simeq 500 \text{ km.s}^{-1}$ , then, assuming that the time for a photon to go around the universe can be estimated by  $t \simeq r_+/c$ , one obtains the maximal precision on the determination of position  $\delta\chi \simeq (v_p/c) \times r_+$ .
- (iii) morphology: when one tries to associate two images to the same physical object, one has to be aware that, in general, the object will not be seen in the same angle and at the same stage of its evolution. It will then be very difficult to recognise it and the identification will strongly depend on galactic evolution models.

Conversely, the discovery of topology by any means could provide informations such as peculiar velocities with a better accuracy [75]. We will also be able to see the same object at different stages of its evolution and on different angles, which will constrain galactic evolution models.

### 2.3. The crystallographic method

Since there is little chance to recognise different images of a given object, one can try to detect these images statistically, since for instance the number of topological images of a single object in a toroidal universe has been estimated in table 1 of [64].

The crystallographic method [64] is based on a property of multi-connected universes according to which each topological image of a given object is linked to each other one by the holonomies of space. Indeed, we do not know these holonomies as far as we have not determined the topology, but we know that they are isometries. For instance in locally Euclidean universes, to each holonomy is associated a distance  $\lambda$ , equal to the length of the translation by which the fundamental domain is moved to produce the tessellation in the covering space. Assuming the FP contains  $N$  objects (e.g. galaxy clusters), if we calculate the mutual 3D-distances between every pair of

### Number of topological images of a single object

$L$	$N(z < 1000)$	$N(z < 4)$	$N(z < 1)$
500	7000	1200	180
1500	279	45	7
2500	60	10	1.5

**Table 1.** Number of topological images of a single object in a toroidal universe with characteristic size  $L$  (in  $h^{-1}$  Mpc). Reprinted from Lehoucq *et al.* [64].

topological images (inside the particle horizon), the distances  $\lambda$  will occur  $N$  times for each copy of the fundamental domain, and all other distances will be spread in a smooth way between zero and two times the horizon distance. In a histogram plotting the number of pairs versus their 3D separations, the distances  $\lambda$  will thus produce spikes. Simulations indeed showed that the pairs between two topological images of the same object drastically emerge from ordinary pairs [64] in the histogram. The applicability of the method in Euclidean spaces has also been discussed by Fagundes and Gaussmann [63] when the size of the physical space is comparable to the horizon size.

Two kind of catalogs of astronomical objects can be thought of to apply this method: the galaxy cluster catalogs, which typically have a redshift depth  $z = 1$ , and the quasars catalogs, which typically extend to  $z = 3$ . Concerning quasars, even if their lifetime is probably too short to be good candidates for producing topological images, they are usually part of systems that have a much larger lifetime [65]. Let us stress that a recent survey [66] in the Hubble Deep Field south NICMOS field found 17 galaxies with a redshift between 5 and 10 and 5 galaxies with a redshift above 10, among a total of 323 galaxies. This can let us hope to apply this method to deeper catalogs in the future. The angular resolution needed is given by the fact that the objects have a peculiar velocity and that they will not be seen at exactly the same position [33]. Note that the crystallographic method, contrary to the “direct” method which would try to recognize topological images of individual objects, is not plagued by the fact that topological images of the same object are seen at different stages of its evolution.

We present on figure 2 an example from [64] for the flat torus with a cubic FP.

Now, we apply this method to a catalog [76] containing more than 11,000 quasars up to a redshift of  $z \simeq 3.25$  (see figure 3 where we have depicted its projection on the celestial sphere and the redshift distribution of its objects). The pair separation histogram is plotted on figure 4 and it exhibits no topological signature. Since respectively 60 %, 80 % and 95 % of the sources are below the redshifts 2, 2.3 and 3, we only test scales smaller than  $z \simeq 3$ .

In a locally Euclidean universe, the distance-redshift relation is given by [77]

$$\chi(z) = \frac{2c}{a_0 H_0} \left( 1 - \frac{1}{\sqrt{1+z}} \right). \quad (11)$$

We simulated a catalog with the same number of objects and the same redshift distribution to reproduce the real catalog depicted in figure 3. Varying the size of

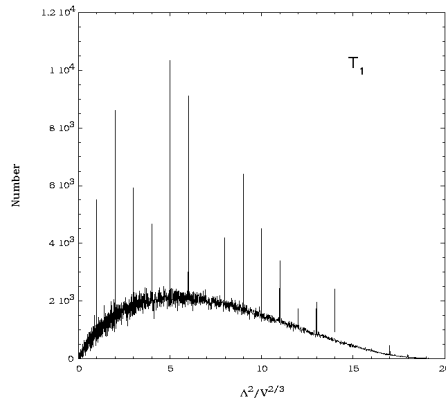


**Figure 2.** Application of the crystallographic method in a cubic torus universe, from [64]. Here,  $\Lambda$  corresponds to the separation distance and  $V$  to the volume of the manifold.

cubic hypertorus, a spike appears when  $L_0 \simeq 3000 h^{-1}$  Mpc for the simulated catalog and thus we obtain the new bound on the size of a locally Euclidean manifold as

$$L_0 \geq 3000 h^{-1} \text{ Mpc}, \quad (12)$$

which is the best constraint presently available with 3D-methods for locally Euclidean manifolds. Note that it corresponds to

$$\frac{L_0}{R_H} \geq 0.5, \quad (13)$$

which is comparable to the bound obtained with 2D-methods. Note that this result has not been published elsewhere.

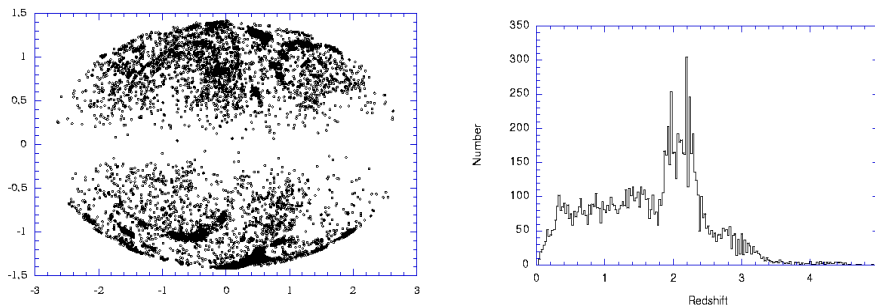


**Figure 3.** The quasar catalog: (left) the distribution of objects on the celestial sphere in Hammer–Aitoff equal area projection and (right) the redshift distribution.

### 3. WHY THE CRYSTALLOGRAPHIC METHOD DOES NOT WORK IN HYPERBOLIC SPACES

When one looks carefully at the crystallographic method, one must wonder about the origin of the spikes. As it has recently been explained [67], two kinds of pairs can

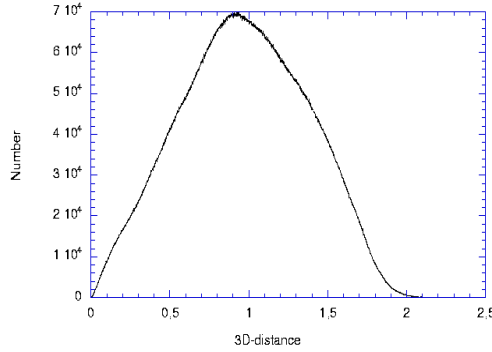


**Figure 4.** The pair separation histogram for the quasar catalog (see figure 3) exhibits no topological signature when assuming a locally Euclidean geometry.

create a spike, namely (we keep the notation and vocabulary introduced in [67])

- (i) *Type I pairs* of the form  $\{g(x), g(y)\}$ , since  $\text{dist}[g(x), g(y)] = \text{dist}[x, y]$  for all points and all elements  $g$  of  $\Gamma$ .
- (ii) *Type II pairs* of the form  $\{x, g(x)\}$  if  $\text{dist}[x, g(x)] = \text{dist}[y, g(y)]$  for at least some points and elements  $g$  of  $\Gamma$ .

Both families of pairs are depicted on figure 5 for the example of the 2-torus.

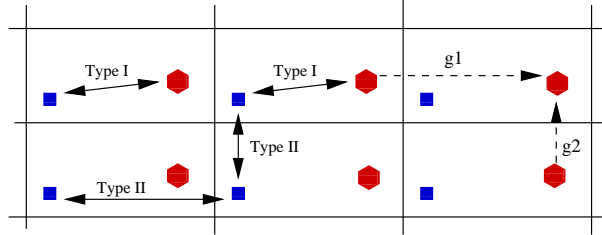


**Figure 5.** Difference between type I and type II pairs in the example of the two dimensional torus. The translations  $g_1, g_2, g_1^{-1}$  and  $g_2^{-1}$  are the generators of the holonomy group. Type I pairs are the ones between the ghosts of two distinct objects (hexagon or square), and type II pairs are the ones between two topological images of the same object.

### 3.1. Clifford translations

A Clifford translation is an isometry  $g$  such that the displacement function  $\text{dist}(x, g(x))$  is constant [19]. This is precisely what is required to get type II pairs in the histogram.

In compact hyperbolic manifolds,  $\text{dist}[x, g(x)]$  always depends on the position  $x$  of the source (see [67] for details).

In elliptic spaces, distances are position-independent whenever the holonomy is a Clifford translation. All finite groups of Clifford translations of spheres are the cyclic group, the binary dihedral, tetrahedral, octahedral and icosahedral groups [69], from

which we deduce [67] that the covering transformations which move a source to its nearest neighbours are Clifford translations (although the transformations to more distant neighbours might not be), and type II pairs can be produced.

In locally Euclidean universes, type I and type II pairs are both present. The reason is that the 3-torus has the very special property that the separation distance of gg-pairs (i.e. any pair of images comprising an original and one of its ghosts, or two ghosts of the same object) is independent of the location of the source. In other Euclidean spaces the spectrum of gg-pair distances varies with the location of the source. However all closed Euclidean 3-manifolds have the 3-torus as a covering space, so for each such manifold there will be some distances which are independent of the location of the source. As a consequence, the topological signal expected in the histogram from type I and type II pairs clearly stands out, as was shown in the simulations of [64].

In conclusion, type II pairs exist only in elliptic and Euclidean universes. The question we still have to answer to judge the efficiency of the crystallographic method in the general case is: what about the amplitude of the spikes related to type I pairs only ?

### 3.2. Cosmological parameters

If the injectivity radius of the space manifold is smaller than the catalog's length scale, type I pairs will always be present, whatever the curvature. Their number roughly equals the number of copies of the fundamental domain within the catalog's limits. Following [67], this number can easily be estimated by computing the ratio between the volume of the geodesic sphere of radius  $\chi(z)$  and the volume of the manifold. The calculation (in the case of hyperbolic universes) leads to

$$N(\Omega_{m0}, \Omega_{\Lambda0}; z < Z) = \frac{\pi (\sinh 2\chi(Z) - 2\chi(Z))}{\text{Vol}(\Sigma)}, \quad (14)$$

where  $\chi(Z)$  is the radial distance corresponding to the redshift  $Z$ , given

$$\chi(z) \equiv \int_{a_0}^a \frac{da}{a\dot{a}} = \int_{\frac{1}{1+z}}^1 \frac{\sqrt{1 - \Omega_{m0} - \Omega_{\Lambda0}} dx}{x \sqrt{\Omega_{\Lambda0} x^2 + (1 - \Omega_{m0} - \Omega_{\Lambda0}) + \frac{\Omega_{m0}}{x}}}, \quad (15)$$

where  $\Omega_{m0}$  and  $\Omega_{\Lambda}$  are respectively the density parameter and the cosmological constant. We have plotted on figure 6 an estimation of the number of copies of an object taken respectively in a catalog of galaxy clusters and in a catalog of quasars, as a function of the cosmological parameters.

The small number of type I pairs in hyperbolic manifolds is due to the property that the volume of the manifold is fixed once the topology is determined (the *rigidity theorem*), contrarily to Euclidean spaces where the characteristic sizes and the volume of the FP can be chosen at will (since  $K = 0$ , the geometry does not impose any characteristic size).

In conclusion, type I pairs will indeed contribute to spikes in the pair separation histogram but the amplitude of these spikes will be of the same order than the statistical noise.

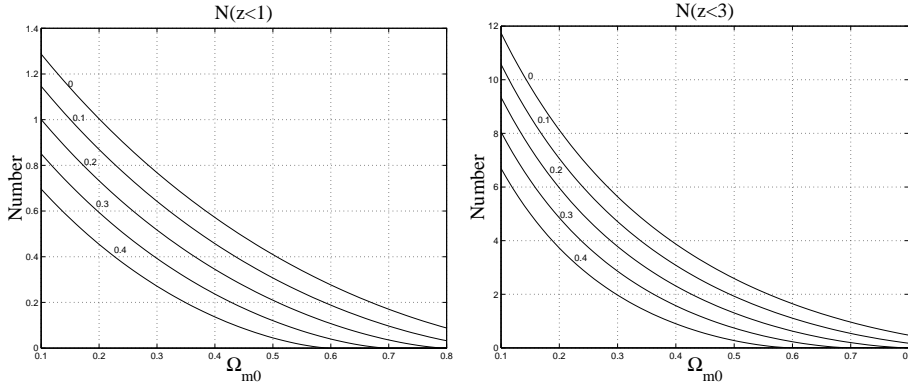


**Figure 6.** The number of copies of an object belonging to a catalog of clusters (left) and a catalog of quasars (right) as a function of the cosmological parameters.

### 3.3. Numerical simulations

The former conclusion can be tested numerically. For that purpose, we concentrate on locally hyperbolic three-dimensional manifolds. It can be first embedded in a four-dimensional Minkowski space by introducing the set of coordinates  $(x^\mu)_{\mu=0..3}$  related to the intrinsic coordinates  $(\chi, \theta, \varphi)$  through (see e.g. [69, 70])

$$\begin{aligned}
 x_0 &= \cosh \chi \\
 x_1 &= \sinh \chi \sin \theta \sin \varphi \\
 x_2 &= \sinh \chi \sin \theta \cos \varphi \\
 x_3 &= \sinh \chi \cos \theta,
 \end{aligned} \tag{16}$$

so that the three-dimensional hyperboloid  $H^3$  has the equation

$$-x_0^2 + x_1^2 + x_2^2 + x_3^2 = -1. \tag{17}$$

With these notations, the comoving spatial distance between two points of comoving coordinates  $x$  and  $y$  can be computed directly in the Minkowski space by [71]

$$d[x, y] = \arg \cosh [x^\mu y_\mu], \tag{18}$$

where  $x_\mu = \eta_{\mu\nu} x^\nu$ ,  $\eta_{\mu\nu}$  being the Minkowskian metric coefficients.

To generate an idealised catalog,  $\mathcal{C}$ , we first distribute *homogeneously*  $N$  objects in the FP, then we by unfold the catalog by applying the generators of the holonomy group. Now, to generate a catalog with the required depth  $z_{\max}$  in redshift, the set of all points obtained as above must be truncated in order to keep only the points  $x$  such that  $\text{dist}[0, x] \leq \chi(\Omega_{m0}, \Omega_{\Lambda0}; z_{\max})$ , given by equation (15). This amounts to select objects located within the geodesic ball of radius  $\chi(\Omega_{m0}, \Omega_{\Lambda0}; z_{\max})$  centered onto an observer right at the centre.

The unfolding of Weeks manifold is shown in figure 7, where we have depicted the central cell and its 18 nearest neighbours in Klein coordinates. In figure 8, we have plotted a simulated catalog showing all points, including those outside the horizon distance.

We then compute all the 3D separations between all the pairs of  $\mathcal{C}(z)$  and we plot the histogram of the number of pairs with a given separation.

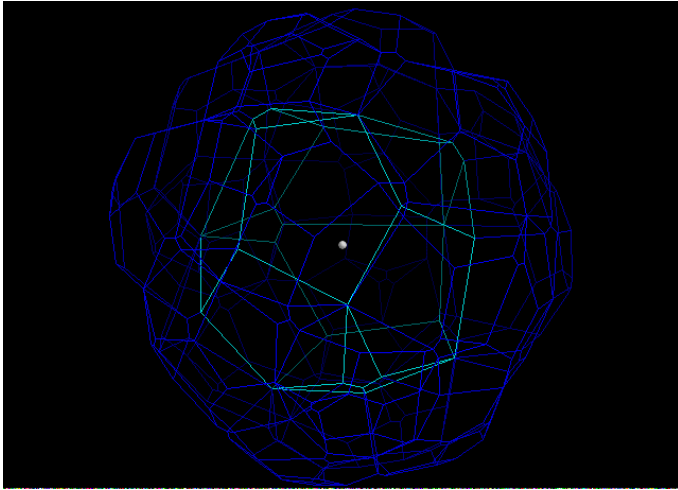


**Figure 7.** Unfolding the Weeks manifold: we have represented the FP and its 18 nearest copies in Klein coordinates.

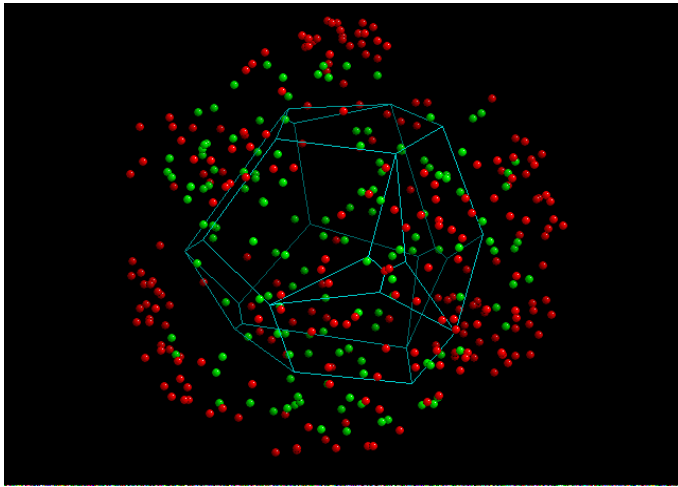


**Figure 8.** Building a catalog  $\mathcal{C}$  for the Weeks manifold. The green dots are objects located within the horizon. The red ones lie outside and will be rejected from  $\mathcal{C}$ .

Indeed the former procedure applies when the observer stands at the center of the polyhedron ( $\chi = 0$ ). In [67], we explain how to take into account an off-centered observer.

In Lehoucq et al. [67], we have generated some pair histograms in a universe whose spatial sections have the topology of the Weeks manifold, using  $N = 1000$  objects in the FP. In figure 9 we give an example when  $\Omega_\Lambda = 0$ ,  $\Omega_{m0} = 0.2$  and where the observer stands at the center of the polyhedron ( $\chi = 0$ ). The dependence on the cosmological parameters, on the position of the observer and on the catalog depth where studied in details in [67].

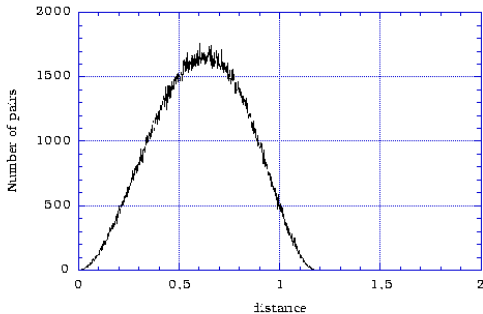


**Figure 9.** Pair separation histogram for a universe with the topology of the Weeks manifold,  $\Omega_0 = 0.2$ ,  $\Omega_\Lambda = 0$ , for a simulated catalog of cosmic objects with depth  $z_{\max} = 1$ . No spike stands out.

As expected, none of the plots exhibit spikes. This is due to the combined effects of the geometry and of the cosmological parameters values.

To summarize the failure of cosmic crystallography for hyperbolic manifolds:

- (i) hyperbolic manifolds are such that  $\text{dist}[x, g(x)]$  depends on  $x$ , so that there is no amplification for the *type II pairs*  $\{x, g(x)\}$ , whereas  $\text{dist}[x, g(x)] = \text{dist}[y, g(y)]$  in the Euclidean case. This suppresses the corresponding spikes.
- (ii) The spikes associated to the isometries (i.e. such that  $\forall g \in \Gamma, \text{dist}[g(x), g(y)] = \text{dist}[x, y]$ ) must remain. But, given the cosmological parameters, we have shown that the number of topological images is too low to create such spikes associated to *type I pairs*.

#### 4. GENERALISING THE CRYSTALLOGRAPHIC METHOD

The next question is: can we generalise the crystallographic method in order to make it work in any case ?

Two solutions were proposed almost immediately to improve the crystallographic method and to extract from 3D catalogs the signature of type I pairs:

- (i) Fagundes and Gaussman [72] subtracted the pair separation histogram for a simulated catalog (with the same number of objects and the same cosmological parameters) in a simply-connected universe to the observed pair separation histogram. The result is “a plot with much oscillation on small scale, modulated by a long wavelength quasi-sinusoidal pattern”. The statistical relevance of this signature still has to be investigated. To illustrate this point we show on figure 10 the result of a simulation where we have subtracted to realisations on a simply-connected Friedmann-Lemaitre universe. This has to be compared with figure 1 from [72] and let us think that is method is not efficient for determining a relevant signature of the topology of the universe.
- (ii) Gomero *et al.* [68] proposed to split the catalog in “smaller” catalogs and average the pair separation histograms built from each sub-catalog to reduce the statistical noise and extract a visible signal of the non-translational isometries. The feasibility of this method has not yet been demonstrated.

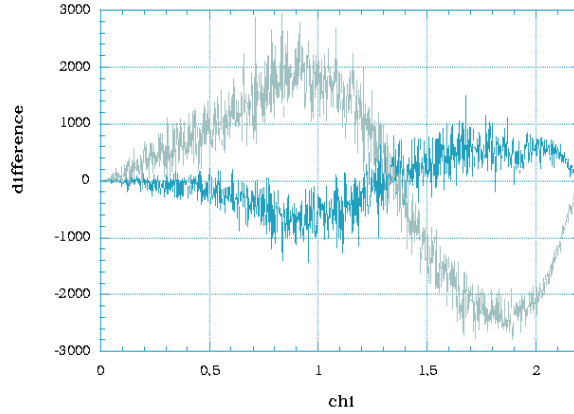


**Figure 10.** The plot for the Weeks manifold [grey] compared to the difference between two realisations in simply-connected universes with same local geometry [green].

## 5. A NEW EFFICIENT STATISTICAL METHOD

We now present a new method [73] based on the property that whatever the topology, type I pairs will always exist. Indeed, as shown ahead, this does not lead to any observable spike in the pair separation histogram. We thus had to find a method to enhance the topological signal by “collecting” all the homologous pairs together. This can be achieved by building a *collecting correlated pairs* method (hereafter *CCP*). Such an approach (described in details in [73] and below) is not able to determine the exact topology, but will provide a signature of the compactness of the spatial sections, which is indeed a first step toward the determination (or the rejection) of the cosmic topology.

In this section, we recall the construction of the CCP-index and the main results we have obtained.

### 5.1. Basic idea and general method

As stressed in the previous section, type I pairs will always exist in multi-connected spaces as soon as one of the characteristic scales of the fundamental domain is smaller than the Hubble scale. Defining  $g_i|_{1 \leq i \leq 2K}$  as the  $2K$  generators of  $\Gamma$  and referring to  $x$  as the position of the image in the universal covering space  $X$ , we have:

$$(i) \quad \forall x, y \in X, \forall g \in \Gamma,$$

$$\text{dist}[g(x), g(y)] = \text{dist}[x, y]. \quad (19)$$

We will refer to these pairs as  $xy$ -pairs.

$$(ii) \quad \forall x \in X, \forall g_1, g_2 \in \Gamma,$$

$$\text{dist}[g_1(x), g_1 \circ g_2(x)] = \text{dist}[x, g_2(x)]. \quad (20)$$

We will refer to these pairs as  $xg(x)$ -pairs.

Both the  $xy$ -pairs and the  $xg(x)$ -pairs are type I pairs.

To collect all these pairs together and enhance the topological signal, we define the *CCP-index* of a catalog containing  $N$  objects as follows.

- (i) We compute all the 3D-distances  $\text{dist}[x, y]$  for all points within the catalog's limit.
- (ii) We order all these distances in a list  $d_i|_{1 \leq i \leq P}$ , where  $P \equiv N(N-1)/2$  is the number of pairs, such that  $d_{i+1} \geq d_i$ .
- (iii) We create a new list of increments defined by

$$\forall i \in [1 \dots P-1], \quad \Delta_i \equiv d_{i+1} - d_i \quad (21)$$

(keeping all the equal distances, if any, in the list).

- (iv) We then define the CCP-index  $\mathcal{R}$  as

$$\mathcal{R} \equiv \frac{\mathcal{N}}{P-1}, \quad (22)$$

where  $\mathcal{N} \equiv \text{card}(\{i, \Delta_i = 0\})$ , so that  $0 \leq \mathcal{R} \leq 1$ .

With such a procedure, all type I pairs will contribute to  $\mathcal{N}$ . For instance, if a given distance appears 4 times in the list  $d_i|_{1 \leq i \leq P}$ , it will contribute to 3 counts in  $\mathcal{N}$ . Compared to the old crystallographic method, all the correlated pairs are gathered into a single spike, instead of being smoothed out into the noise of the histogram pair separation.

Indeed, in a more realistic situation, one has to take into account bins of finite width  $\epsilon$  and replace  $\mathcal{N}$  by

$$\mathcal{N}_\epsilon \equiv \text{card}(\{i, \Delta_i \in [0, \epsilon]\}) \quad (23)$$

in the computation of  $\mathcal{R}$ . The effect of this ‘‘binning’’ is discussed below. We now focus on the ‘‘idealised’’ version of the procedure by studying the amplitude of the CCP-index in some multi-connected models.

For that purpose, let us assume that the catalog is obtained from an initial set of  $A$  objects lying in the fundamental domain and that  $B$  copies of the domain are within the catalog's limits ( $B = 0$  if the whole observable universe up to the catalog's limit is included inside a fundamental domain). The total number of images is  $N = A(B+1)$ . Indeed  $B$  is usually not an integer but we assume it is, in order to estimate the amplitude of  $\mathcal{R}$  and compare it with the result in a simply-connected model. In [73], it has been shown that

$$\mathcal{N}_{\min} = A \left[ (A-1) \frac{B}{2} + A\nu_1(\Sigma, B) \right], \quad (24)$$

where  $\nu_1(\Sigma, B)$  is a function characterising the manifold  $\Sigma$ . It is an increasing function of  $B$  which vanishes for  $B = 0$ .

Indeed, if the holonomy group  $\Gamma$  contains Clifford translations allowing for type II pairs, or if there are ‘‘fake’’ pairs (i.e. such that  $\text{dist}[x, y] = \text{dist}[u, v]$ ),  $\mathcal{N}_{\min}$  computed from (24) will give a lower bound for the true  $\mathcal{N}$ .

The normalised CCP-index (22) follows straightforwardly.  $\mathcal{R}$  is a good index for extracting the topological signal since

- (i) when  $B = 0$  (i.e. when the fundamental domain is greater than the catalog's spatial scale),  $\mathcal{R} = 0$ ,
- (ii) when the number of sources in the fundamental domain becomes large, it behaves as

$$\mathcal{R} \rightarrow \frac{B + 2\nu_1(\Sigma, B)}{(B + 1)^2} \quad \text{as } A \rightarrow \infty. \quad (25)$$

As shown in [73], one can compute analytically the CCP-index in various examples and show that it is a fair indicator of the existence of at least one compact spatial dimension.

## 5.2. Simulations and statistical relevance

Now that the CCP-index can be computed for any multi-connected space, we can compare it with its value in a simply-connected Friedmann-Lemaitre model containing the same number objects (i.e.  $A(B+1)$ ).  $\mathcal{R}$  is given as a function of  $\nu_1$ ,  $A$  (the number of sources in the fundamental domain) and  $B$  (the number of copies of the domain within the observable universe) by:

$$\mathcal{R} = \frac{A[(2\nu_1 - B)A - B]}{(B + 1)^2 A^2 - (B + 1)A - 2}. \quad (26)$$

Indeed, when working with a real catalog, we do not know the radial distance of cosmic objects but only their redshift. As seen before, the determination of the radial distance requires the knowledge of the cosmological parameters  $\Omega_0$  and  $\Lambda$  and can be obtained analytically only when  $\Lambda = 0$ .

Thus, if the universe is multi-connected on sub-horizon scale, the plot of  $\mathcal{R}$  in terms of  $\Omega_0$  and  $\Omega_\Lambda$  will exhibit a spike only when the cosmological parameters have the right value (as shown on plot 7 of [73]). If the cosmological parameters are not exactly known, the distance determination (15) will be wrong and the topological signature will be destroyed (see figure 6 in [73]).

Two consequences follow:

- (i) One should span the parameters space  $(\Omega_0, \Omega_\Lambda)$  in order to detect the topological signal, plotting  $\mathcal{R}(\Omega_0, \Omega_\Lambda)$ .
- (ii) If there is any topological signal, the position of the spike gives the values of the cosmological parameters on the scale of the catalog's limit (see figure 11).

We proceed as follows. We first generate a catalog by choosing the number of objects in the fundamental domain ( $A = 30$ ), the topology (Weeks manifold) and the cosmological parameters (e.g.  $\Omega_0 = 0.2$ ,  $\Omega_\Lambda = 0.1$ ), we then use a second code to apply the test and we draw  $\mathcal{R}$  in terms of the two cosmological parameters. As shown in [73], the method works pretty well in the sense that there is a strong spike which signals a non trivial topology and which determines the cosmological parameters. But we also see that a slight deviation in the evaluation of the cosmological parameters would make the spike to disappear. This effect is now discussed.

### 5.3. Real data

When one wants to apply the CCP-method to real data, one has to face a number of problems.

First, we cannot use a zero width bin, one of the reasons being that the sources are not comoving. In [73], we estimate the precision needed on the cosmological parameters when working with a bin width  $\epsilon$  such that

$$\left| \frac{\delta\Omega_0}{\Omega_0} \right| \simeq \epsilon. \quad (27)$$

Indeed, using a catalog with a smaller depth  $z_{\max} = 3$  will allow us to use a smaller resolution for the cosmological parameters. One has thus to find a compromise between depth and resolution as discussed in [73]. On figure 11, we give an example with a bin width of  $\epsilon = 10^{-6}$  which produces a background noise.

Now, we apply our test to the quasars catalog [76] used ahead (see figure 3). No topological signature was found [73]. Does it mean that there is no topological effect on scales smaller than  $z_{\max} \simeq 3$ ? Not necessarily, since we applied the test with precisions  $\epsilon = 10^{-7}, 10^{-6}, 10^{-5}$  and were unable to span the full cosmological parameters' space with the required accuracy. The computational time is one of the main limitations of our technique (this point is discussed extensively in [73])

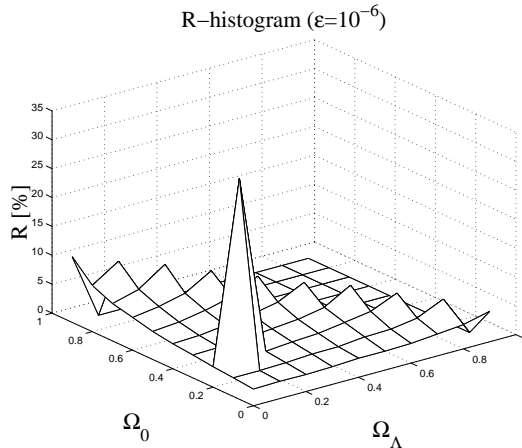


**Figure 11.** Computation of the CCP-index on a simulated catalog of depth  $z = 3$  in a universe model with the Weeks topology,  $\Omega_0 = 0.2$ ,  $\Omega_\Lambda = 0.1$ , using a bin resolution  $\epsilon = 10^{-6}$ .

Now, another limitation comes from the peculiar velocities of the sources. In [73], we discussed in details the effect of peculiar velocities both on  $xy$ -pairs and on  $xg(x)$ -pairs, we and showed that even if the amplitude of the topological signal is reduced, it is not destroyed.

## 6. CONCLUSIONS

We have reviewed the main allowed topological structures for relativistic universe models and we discussed the various methods aimed to detect this topology. Focusing on 3D-methods, we described the crystallographic method and we applied it to

a quasars catalog to obtain a new constraint for Euclidean manifolds,  $L_0 \geq 3000 h^{-1}$  Mpc. Then we discussed the failure of this method for detecting the topology of compact hyperbolic manifolds. We thus generalised the method by introducing a new technique based on the construction of a CCP-index. The main difference with the cosmic crystallography method is the collecting process of all correlated pairs of the catalog, which enhances the signal associated to the existence of a non trivial topology. We gave examples of computation of such an index in order to show its statistical relevance. We finally discussed the implementation difficulties of this new method when working with observational data.

## References

- [1] A.A. Friedmann, Zeitschr.für Phys. **21** (1924) 326
- [2] A. Einstein, Preuss. Akad. Wiss., Sitzungsber. (1917) 142.
- [3] W. de Sitter, Mon. Not. R. Astron. Soc. **78** (1917) 3.
- [4] H. Olbers, *La transparence de l'espace cosmique* (1823); Traduction J. Merleau-Ponty in *L'univers à l'âge du positivisme*, 319 (1983) Eds. Vrin, Paris.
- [5] E. Mach, *Conservation of energy* (1872); Traduction E. Bertrand, Ed. Hermann, Paris (1904).
- [6] E. Mach, *The science of mechanics* (1883). (new edition Open Court Publishing Company, Illinois, 1902).
- [7] Epicure, *Letter to Herodotus*
- [8] G.F.R. Ellis, Gen. Rel. Grav. **2** (1971) 7.
- [9] J.A. Wheeler, Ann. Phys. **2** (1957) 604.
- [10] D. Aktaz et H. Pagels, Phys. Rev. **D25** (1982) 2065.
- [11] S. Hawking, Nucl. Phys. **B239** (1984) 257.
- [12] G.W. Gibbons, Class. Quant. Grav. **15** (1998) 2605.
- [13] E. Feodoroff, Russian Journ. for Crystallography and mineralogy **21** (1885) 1.
- [14] L. Bierberbach, Mathematische Annalen **70**, (1911) 297; *Ibid*, **72** (1912) 400.
- [15] W. Novacki, Commentarii Mathematici Helvetici **7** (1934) 81.
- [16] F. Klein, Mathematisches Annalen **37** (1890) 1.
- [17] W. Killing, Mathematisches Annalen **39** (1891) 1.
- [18] J.A. Wolf, Comptes rendus de l'Académie des Sciences de Paris **250** (1960) 3443.
- [19] W.P. Thurston *The geometry and topology of three manifolds*, Princeton Lecture Notes (1979).
- [20] W.P. Thurston and J.R. Weeks, Sci. Am., July, 94 (1984).
- [21] J. Weeks, *The shape of space: how to visualize surfaces and three dimensional manifolds*, M. Dekker, New-York (1985).
- [22] W.P. Thurston, *Three-dimensional geometry and topology* Vol. 1 (1997) Princeton Methematical series 35, Ed. S. Levy, Princeton University Press.
- [23] W.P. Thurston, Class. Quant. Grav. **15** (1998) 2545.
- [24] J-P. Luminet, Proceedings of "Concepts de l'Espace en Physique", Les Houches, 29 sept - 3 oct 1997 (1998), to appear in Acta Cosmologica, [gr-qc/9804006].
- [25] J-P. Luminet, J-P. Luminet, B.F. Roukema, proceedings of Cargese summer school "Theoretical and Observational Cosmology", Cargese, Corsica, August 1998 [astro-ph/9901364].
- [26] J-P. Luminet, *A. Friedmann, G. Lemaitre : Essais de Cosmologie*, précédés de *L'invention du Big-bang*, Ed. Seuil, Collection "Source du savoir" (1997).
- [27] J.-P. Luminet, G. Starkman, J. Weeks, Scientific American, april 1999, **280** 90.
- [28] R. Geroch, Proc. Int. Scool of Physics 'Enrico Fermi', course XLVII, ed. R.K. Sachs, NY academic Press (1971) 104.
- [29] S. Hawking and G.F.R. Ellis *Large scale structure of spacetime* (1973) Cambridge university Press.
- [30] J.A. Wolf, *Spaces of constant curvature*, Cinquième édition, Publish or Perish Inc., Wilmington USA (1967).
- [31] A.F. Beardon, *The geometry of discrete groups*, New York, Springer (1983).
- [32] M. Nakahara, *Geometry, Topology and Physics*, Adam Hilger, Bristol, New-York (1990).
- [33] M. Lachièze-Rey and J.-P. Luminet, Phys. Rep. **254** (1995) 135.
- [34] J-P. Uzan, Int. Journal of Theor. Physics **36**, (1997) 2167 .
- [35] J-P. Uzan, *Défauts topologiques et conditions aux limites en cosmologie primordiale*, thèse de l'université Paris XI (1998) [chapters 8-10], [<http://milak.irfu.se/~uzan/pub.html>].

- [36] W.P. Thurston, *Bull. Am. Math. Soc.* **6**, 357 (1982).
- [37] J. Weeks, PhD Thesis, Princeton University (1985).
- [38] S.V. Matveev and A.T. Fomenko, *Russian Math. Surveys* **43** (1988) 3.
- [39] J. Weeks: <http://www.geom.umn.edu:80/software>.
- [40] G.D. Mostow, *Ann. Math. Studies* **78** (1973) Princeton University Press.
- [41] G. Prasad, *Invent. Math.* **21** (1973) 255.
- [42] D. Gabai, G.R. Meyerhoff and N. Thurston, MSRI preprint 1996-058 (1996).
- [43] K. Schwarzschild, *Vierteljahrsschrift der Astr. Ges.* **35** (1900) 337; English translation in *Class. Quant. Grav* **15** (1998) 2539.
- [44] Proceedings of the workshop *Cosmology and topology*, Cleveland 25-27 october 1997, *Class. Quant. Grav.* **15**(1998).
- [45] B.F. Roukema, *Month. Not. R. Astron. Soc.* **283** (1996) 1147.
- [46] B.F. Roukema and A.C. Edge, *Month. Not. R. Astron. Soc.* **292** (1997) 105.
- [47] D. Stevens, D. Scott and J. Silk, *Phys. Rev. Lett.* **71** (1993) 20.
- [48] A. de Oliveira Costa, G.F. Smoot and A.A. Starobinsky, *Astrophys. J.* **468** (1996) 457.
- [49] N.J. Cornish, D.N. Spergel and G.D. Starkman, *Phys. Rev.* **D57** (1998) 5982.
- [50] J. Levin, E. Scannapieco, G. de Gasperis, J. Silk and J.D. Barrow, [[astro-ph/9807206](mailto:astro-ph/9807206)].
- [51] J. Levin, E. Scannapieco and J. Silk, *Class. Quant. Grav.* **15** (1998) 2689; *ibid.* *Phys.Rev.* **D58** (1998) 103516.
- [52] K.T. Inoue, [[astro-ph/9810034](mailto:astro-ph/9810034)].
- [53] J.R. Bond, D. Pogosyan and T. Souradeep, *Class. Quant. Grav.* **15** (1998) 2671.
- [54] J-P. Uzan and P. Peter, *Phys. Lett.* **B406** (1997) 20.
- [55] J.P. Uzan, *Phys. Rev.* **D58** (1998) 087301; *ibid.*, *Class. Quant. Grav.* **15** (1998) 2711.
- [56] R. Aurich, [[astro-ph/9903032](mailto:astro-ph/9903032)].
- [57] L.Z. Fang and H. Sato, *Comm. Theoret. Phys. (China)* **2** (1983) 1055.
- [58] D.D. Sokolov and V.F. Shvartsman, *Sov. Phys. JETP* **39** (1974) 196.
- [59] T. Fetisova *et al.*, *Astron. Lett.* **193** (1993), 198.
- [60] M. Demianski and M. Lapucha, *Month. Not. R. Astron. Soc.* **224** (1987) 527.
- [61] H.V. Fagundes and W.F. Wichoski, *Astrophys. J.* **322** (1987) L5.
- [62] J.R. Gott III, *Month. Not. R. Astron. Soc.* **193** (1980) 153.
- [63] H.V. Fagundes and E. Gaussman, [[astro-ph/9704259](mailto:astro-ph/9704259)].
- [64] R. Lehoucq, M. Lachièze-Rey and J-P. Luminet, *Astron. Astrophys.* **313** (1996) 339.
- [65] G. Paál, *Acta. Phys. Acad. Hungaricae* **30** (1971) 51.
- [66] H.W. Chen *et al.*, [[astro-ph/9812339](mailto:astro-ph/9812339)].
- [67] R. Lehoucq, J-P. Luminet and J-P. Uzan, *Astron. Astrophys.*, to appear (1999) [[astro-ph/9810107](mailto:astro-ph/9810107)].
- [68] G.I. Gomerio, A.F.F. Teixeira, M.J. Rebouças and A. Bernui, [[gr-qc/9811038](mailto:gr-qc/9811038)].
- [69] J.A. Wolf, *Spaces of constant curvature*, fifth edition, Publish or Perish Inc., Wilmington USA (1984).
- [70] H.S.M. Coxeter, *Non Euclidean geometry*, University of Toronto Press (1965).
- [71] H.V. Fagundes, *Astrophys. J.* **338**, 618 (1989); *Astrophys. J.* **349** (1960) 678.
- [72] H.V. Fagundes and E. Gaussman, [[astro-ph/9811368](mailto:astro-ph/9811368)].
- [73] J-P. Uzan, R. Lehoucq and J-P. Luminet [[astro-ph/9903155](mailto:astro-ph/9903155)] preprint n° UGVA-DPT 1999/03-1028
- [74] L.A. Best, *Canadian J. Math.* **23** (1971) 451.
- [75] B.F. Roukema and S. Bajtlik, to appear in *Month. Not. R.A.S.* [[astro-ph/9903453](mailto:astro-ph/9903453)].
- [76] catalog n° VII/207 *Quasars and Active Galactic Nuclei* (8th Ed.) (Veron + 1998). Available at <http://cdsweb.u-strasbg.fr/viz-bin/VizieR?-source=VII/207/> via the Centre de Données astronomiques de Strasbourg [<http://cdsweb.u-strasbg.fr/cats/cats.html>].
- [77] P.J.E. Peebles, *Principles of Physical Cosmology*, Princeton University Press (1993).